Tartu University

Faculty of Science and Technology
Institute of Technology

Oleksandr Syzoniuk

A symmetrical DC-to-DC converter for capacitive energy swinging

Master's thesis (30 EAP)
Robotics and Computer Engineering

Supervisor:
Indrek Must
Saoni Banerji

Tartu 2020

ABSTRACT

A symmetrical DC-to-DC converter for capacitive energy swinging

Soft Robotics is a specific robotics subfield that is involved in building robots from highly compliant materials like those found in living organisms. The energy management system is a fundamental aspect of evaluating the energy-autonomy of soft robots.

To date, energy management systems for soft robots with ionic capacitive laminate (ICL) actuators are ineffective and cannot re-use energy, which is irrevocably lost after, each cycle of the robot actuation. Thus, there is a need to provide a suitable energy-conditioning circuit that would allow the re-use of energy between several ICLs at once.

In this thesis, we propose a door to energy management solution through design: asymmetrical bidirectional DC-to-DC converter that could transfer energy between ICLs for prolonged power-autonomous operation.

The proposed solution has the scope to revise the current soft robots in terms of energy management. The idea of increasing energy transfer efficiency will result in efficient soft robots in rescue missions (for instance), that will have a significant impact in the world.

CERCS: T125 Automation, robotics, control engineering

Keywords: supercapacitor, soft robotics, ionic and capacitive laminate, bidirectional DC-to-DC converter, energy management system, energy conditioning circuits

ABSTRACT

Sümmeetriline alalisvoolupendelmuundur mahtuvuslikele süsteemidele

Pehmerobootika on spetsiifiline robootika alamväli, mis tegeleb elusorganismidele sarnaste robotite ehitamisega pehmetest materjalidest. Energiahaldussüsteem on pehmete robotite energeetilise autonoomsuse põhiaspekt. Ioonsest mahtuvuslikust laminaadist (ICL) täituritega pehmerobotite energiahaldussüsteemid on hetkel ebaefektiivsed – nad ei võimalda taaskasutada energiat, mis on saadaval pärast roboti iga töötsüklit. Seega on vaja leida sobiv energiakonditsioneerimislahendus, mis võimaldaks energiat ümber paigutada mitme ICL-i vahel.

Selles lõputöös pakutud disainiga avame uue ukse energiahaldusele: sümmeetriline kahesuunaline DC-DC muundur, mis suudab energiat üle kanda ICL-ide vahel võimaldab ICL-robotitel energiaautonoomselt töötada pikema aja vältel. Kavandatud lahendusel on perspektiiv muuta praeguste pehmerobotite energiahalduslahendusi: energiatõhusad pehmerobotid leiavad rakendust näiteks päästemissioonidel, millel on maailmas oluline mõju.

CERCS: T125 automaatika, robootika, juhtimistehnika

Märksõnad: superkondensaator, pehmerobootika, ioonne ja mahtuvuslik laminaat, kahesuunaline alalisvoolumuundur, energiajuhtimissüsteem, energia konditsioneerimisahelad

Contents

1. Introduction

Soft robotics is a growing field of research that develops highly adaptive robots using the flexibility and adaptability of soft designs. Energy-efficiency and autonomy are essential aspects of their work. The soft robots' energy autonomy depends on the efficiency of the energy management system. Currently, these systems for ICL robots are inefficient and cannot recover energy after a period of activation of the robot. The system can be improved, which in turn will prolong robots' power-autonomous operation.

- Chapter 2

This chapter provides a literature review. It explains the significance of soft robotics. Also in this chapter demonstrates the structure and functions of the ICL robot. The current energy management system is explained, considering aspects of capacitive systems. The current problem related to the irretrievable energy loss for each activation of the robot is described.

- Chapter 3

This chapter describes the main objectives of the thesis. The proposed new energy management system is aimed at designing a symmetrical bidirectional DC-to-DC converter. Special specifications are also defined for the system along with the reasons for the selected topology.

- Chapter 4

In this chapter, the research methodology is presented. Steps of modeling and optimization are given for the symmetrical bidirectional buck-boost DC-to-DC converter to determine optimal parameters that contribute to the system's efficient operation. The operating principle of the proposed system has also been described.

- Chapter 5

The design of the proposed converter is provided in this chapter. The simulation model and the breadboard set up is presented. Also in this chapter shown symmetrical bidirectional buck-boost DC-to-DC operation analysis. The concept of calculating system efficiency is explained. The most efficient energy transfer region is found.

- Chapter 6

This chapter summarizes the study. The obtained results are stated and discussed. Future prospects and possible options for improving the system are set out.

2. Literature Review

2.1. Importance of soft robotics

In recent years, there has been a remarkable advancement in the field of robotics. “Conventional rigid robots are based on a kinematic chain of rigid links that offer robust, fast, and reliable control of robot motion”[1]. Such robots operate perfectly, when necessary, repeat clearly defined movements for mass production. However, they experience an increased level of difficulty to survive in complex unstructured environmental conditions [2]. “One of the primary concerns is the control architectures which rely on pre-programmed motion patterns in conventional robotic systems” [2]. This is exactly when soft robotics emerges as a solution. Having a type of high compliant body structure makes it possible to deform and transform almost in unlimited configurations, which in turn is impossible in the case of traditional rigid robots. Soft robotics employs materials unconventional for robotics, aimed at developing robots that are very similar to living organisms and can imitate biological systems [3]. Soft robotics employs unconventional materials embedding sensing and control architectures that can mimic incredible capabilities of biological organisms in complex tasks [2]. This makes biomimicry one of the precursors of soft robotics [4].

2.1.1. ICL: Structure and Operation

Soft and flexible actuators are needed for a new generation of soft and shape-morphing robots. ICL identifies a class of soft conductive laminates that have simultaneously the best qualities and abilities of an electromechanical actuator and a flexible energy storage unit [5].

ICL has a sandwich structure, which consists of two electrodes immersed in an electrolyte (Figure 2.1). The electrodes are separated by an ion-permeable membrane. The main functions of the membrane are to prevent electronic conductivity and to allow the mobility of ions. The surface charge of an electrode attracts ions of the opposite charge and repels ions of the same charge. With an increase in the partial charge on the electrode surface, the number of ions adsorbed on it also increases [6].

Two charge layers with opposite polarity are formed at the boundary of the electrode and electrolyte. This interfacial region of the surface charge and ions of the opposite charge attracted to it, form an electric double layer (EDL).

Direct activation of ICL is directly related to the amount of charge stored in it. In the presence of voltage between the ICL electrodes made the opposite electrodes to expand or contract in all directions. The remarkably high capacitance per area contributes to high actuation capabilities. The optimal operating voltage of the ICL actuators lies in the range of few volts (similar to that of contemporary electronics) [7].

ICL has a much in common with electric double-layer capacitors (EDLC), and is a capacitive device.

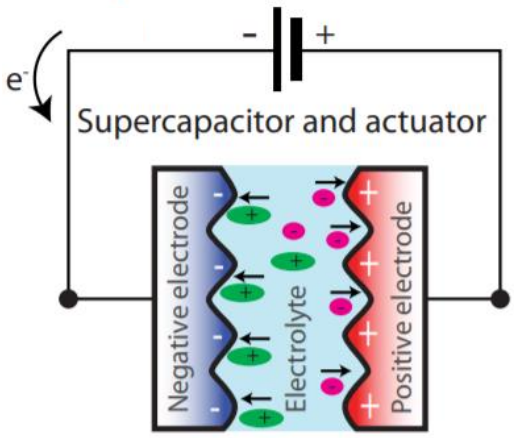

Figure 2.1: ICL structure (adapted from [6])

2.1.2. Electrical equivalent circuits of ICL

An equivalent circuit contributes to understanding the behavior of ICL supercapacitor, as well as its use in a wide range of applications of power electronics. The circuit is shown in Figure 2.2 is an electrical equivalent circuit of ICL which includes capacitance C and equivalent series resistance (ESR)

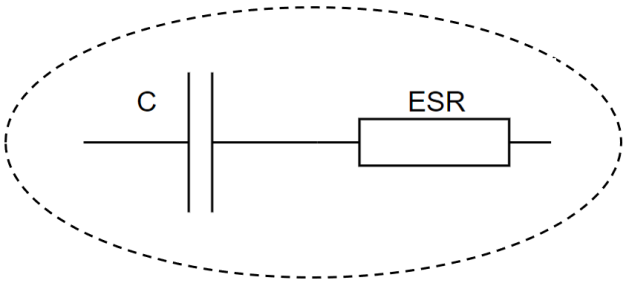

Figure 2.2: ICL electrical equivalent circuit

ESR comes from current collectors, electrode-electrolyte contacts, etc.

Range of ESR for EDLC in 0.01 Ω to 0.5 Ω

The typical value of ESR for ICL is 32 Ω cm^2 [5].

C per area of typical ICL is 150 mF/cm^2 [7]

So we have ESR per C is much higher in ICL than in commercial EDLC.

2.2. Energy efficiency

ICLs are charged using electrical energy from an external source. Although the ICL contains a large amount of electric energy and its charge-storage efficiency can be calculated as $\eta_q = \frac{q_f}{q_i}$, where

η_q is charge storage efficiency, q_f and q_i are final and initial charges respectively. The typical values for η_q can be found in the literature as 84% [6] and 94% [7].

As these ICLs are capacitive, we can also express their corresponding energy storage efficiency as $\eta_E = \frac{E_f}{E_i}$, where η_E is charge storage efficiency, E_f and E_{in} are final and initial energies respectively. The typical values for η_E are 71% for [6] and 88% for [7].

Commercial EDLC charge-storage efficiency very close to 100% without considering energy conditioning circuits. We can conclude, ICL is not nearly as efficient as commercial EDLC, but it still stores a considerable amount of energy reversibly.

2.2.1. Energy management

Energy back up and intermediary storage systems (ISS) are among common use cases for EDLCs. These application areas demand energy conditioning circuits (ECS) not only unidirectional but also bidirectional how shown in Figure 2.3.

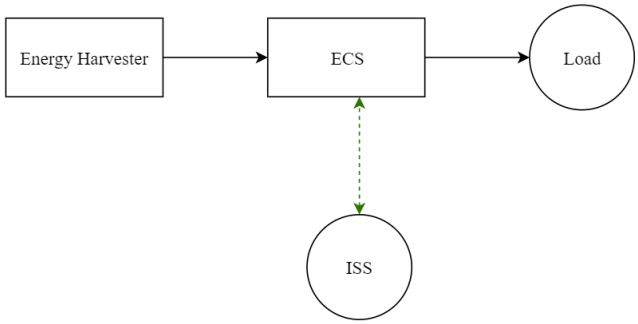

Figure 2.3: Bidirectional Energy Transfer system

In the following sub-section, I give examples of ECS.

2.2.2. DC-to-DC converters

DC-DC converters can be either unidirectional with the ability to transfer energy only in the forward direction from the source to the load, or bidirectional, with the additional possibility of transferring energy from the load back to the source.

Despite the fact that unidirectional converters have found their application in many applications from cellular phones to photovoltaic systems, bipolar converters have not yet reached such widespread use in electronic systems, especially in soft robotics.

Generally, bidirectional DC-DC converters can be divided into two main configuration groups: isolated and non-isolated topologies[8].

In converters with non-isolated topology, energy transition takes place without magnetic isolation. The absence of galvanic isolation in the structure employs a more simplified configuration and reduces the device form factor. This characteristic makes them suitable for the proposed application.

- *Non-isolated bidirectional buck and boost DC-to-DC converter*

The most typical bidirectional converter is a single circuit, antiparallel connected step-down(buck), and step-up(boost) converters [9], as shown in Figure 2.4(a).

This type of converter operates as a step-up converter and boosts voltage from V_L to V_H and performs as a step-down converter and buck voltage, operating in the reverse direction.

The operation of this circuit can be divided into two operating modes, presented as follows. In the forward mode, there is a step-up process, in which the MOSFET S1 (Figure 2.4(a)) performs switching and the MOSFET S2 is turned off (and conduction is happening only through its body diode). In the reverse mode, MOSFET S2 is switched and the circuit operates in step down mode [10]

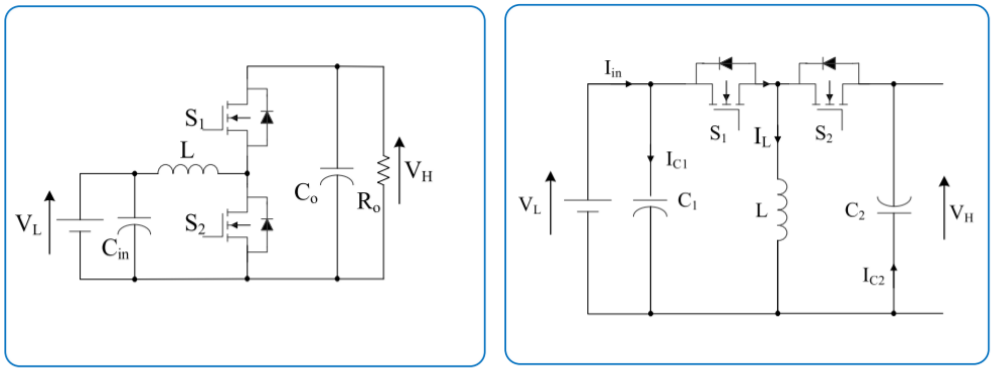

(a) (b)

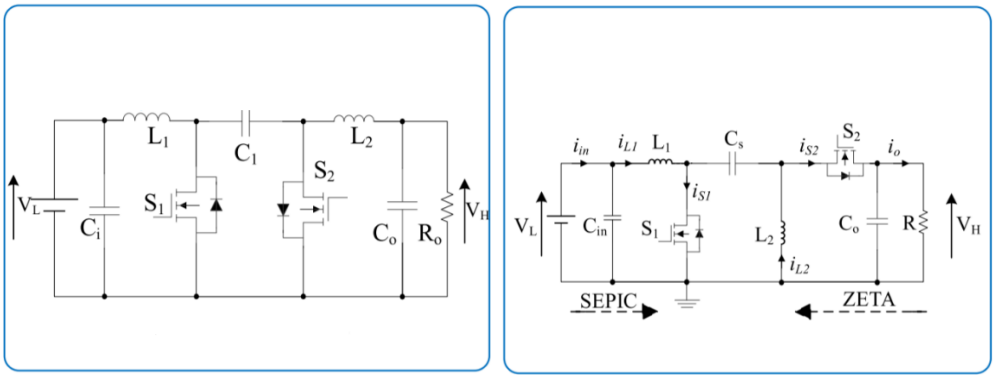

(c) (d)

Figure 2.4: Topologies of the bidirectional DC-DC power converters:

(a) Buck and Boost; (b) Buck-Boost; (c) Cuk; (d) SEPIC/ZETA;

- *Non-isolated bidirectional buck-boost DC-to-DC converter*

The main characteristic of the bidirectional buck-boost converter is its ability to step-up or step-down the voltage level in both directions. The output voltage has a reverse polarity with respect to the input. (Figure 2.4(b)).

When transmitting energy in forward mode, the MOSFET S1 (Figure 2.4(b)) is switched and the MOSFET S2 is off. In the reverse mode, the MOSFET S2 is switched, while the MOSFET S1 is off [9]

- *Non-isolated bidirectional Cuk DC-to-DC converter*

As can be seen from the bidirectional Cuk converter scheme (Figure 2.4(c)), it is a combination of series-connected step up and step-down converters topologies. Additionally, there is an intermediary energy storage capacitor. Since it combines the two previously mentioned topologies, the functional capabilities of this converter also make it possible to have an output voltage value lower or higher than its input voltage. This also applies for converter operation in both directions. When the converter is operating in forward mode, the MOSFET S1 is switched, while the MOSFET S2 is off (and its body diode acts as the main diode). In reverse mode, the MOSFET S2 is switched, while the MOSFET S1 is off [11].

- *Non-isolated bidirectional SEPIC and ZETA DC-to-DC converter*

In general, the SEPIC / Zeta converter circuit is the same Cuk converter with the permutation of two elements. Thus, this converter can also produce both low and high voltage in both directions, without changing polarity of DC buses. When working in the forward mode, SEPIC performs the role of a step-down converter, while working in the reverse mode, ZETA comes into operation and acts as a step-up converter.

2.2.3. Energy management in ICL robots

These ECS can be DC-to-DC converters of different descriptions according to specific use cases.

Such a converter is an electronic device that converts a direct current source (DC) from one voltage level to another [12]. It can act as a bridge for the energy flow between components in one or more directions. Despite the fact that DC-to-DC highly efficient (90%) [13], to-my best knowledge, they have not been implemented in systems with ICL components.

One example of a robot prototype with ICL (Figure 2.5) is a soft robot inspired by inchworm developed in 2014 [5] at the Institute of Technology of Tartu university,

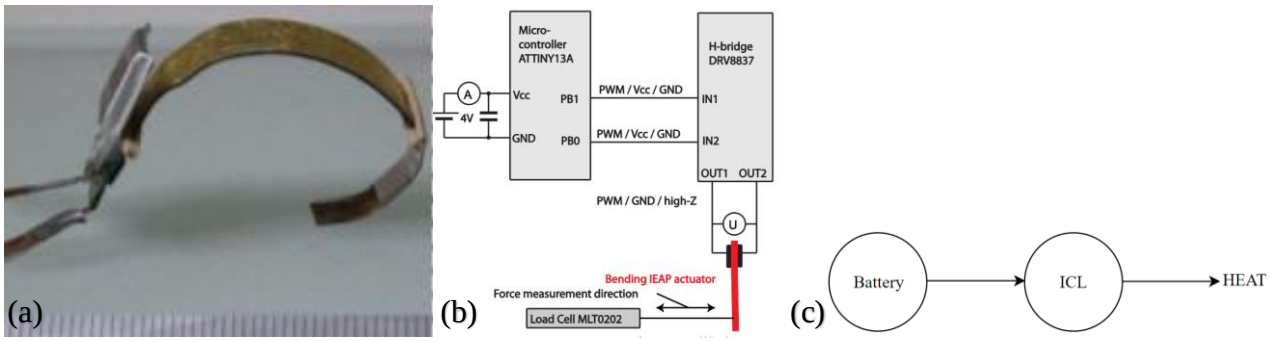

Figure 2.4: Prototype with ICL: (a) Robot [7], (b) Electrical scheme of ICL robot [6], (c) Existing energy flow diagram

The working cycle of the ICL robot consists of a charging period, followed by a short circuit period. During a short circuit, the actuator discharges, resulting in energy loss. Figure 2.5(c) shows a block diagram of energy management in this robot. As we can see, energy is irretrievably spent after each actuation cycle. Such losses are associated with the lack of suitable devices for energy management specific for low voltage capacitive small scale systems.

2.2.4. Energy aspects of capacitive systems

Let's consider a robot with two ICLs with the following constraints for prolonged power-autonomous operation:

- energy-efficiency;
- minimum cost in the weight of the components.

Based on these constraints, could we find a solution just by adding a switch?

This brings us to the so-called "capacitor paradox" (Figure 2.5)

This can be represented as follows:

Let's consider a charged (Q_{c1}) capacitor C1 (with the voltage $U_{c1}=\frac{Qc1}{Cc1}$) connected in parallel to another of equal value (C_{c2}) but uncharged C2 via a switch SW1, as shown in Figure2.2. When the switch SW1 is open, the energy in C1 is:

$$E_{C1} = \frac{1}{2} C_{c1} {U_{c1}}^2 \tag{1.1}$$

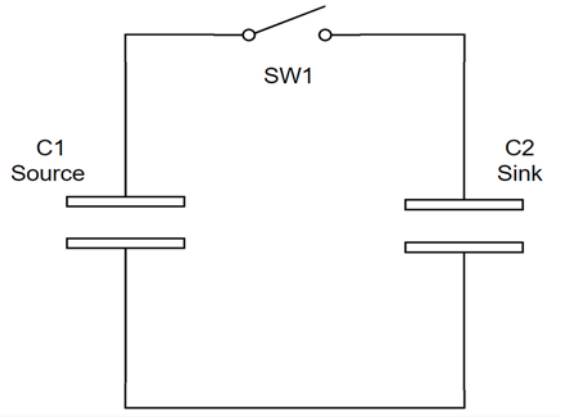

Figure 2.5: Two-capacitor circuit

When the switch SW1 is closed, a part of the charge flows from C1 to C2.

After the switch is closed, the charge is split evenly between the capacitors and both capacitors develop an identical voltage of value $U_f=Q/(C_{c1}+C_{c2})=Q/2C$ which is half of the initial of C1.

The energy in both capacitors is equal, however, we lose energy:

$$E_{total(initial)} = E_{c1} = \frac{Q2}{2C1} \tag{1.2}$$

$$E_{c1(final)} = \frac{Q2}{8C1} = \frac{1}{2}E_{total(initial)} \tag{1.3}$$

Why it appears as a paradox?

From first sight, it is a paradox since we losing energy. However, energy loss cannot be explained by radiation losses or resistive losses. Work done for the charge's expansion accounted for the missing energy. The charge density increase that means charge extant [14].

2.3. Problem statement

Contrary to the two-capacitor circuit in section 2.2.4, in the case of an inductor-capacitor (LC) circuit, energy is transferred between the capacitor and the inductor without energy losses ideally. There is a trade-off between the size and weight of components and efficiency. As we have discussed in section 2.3.2 many DC-to-DC converter topologies intermediary store energy in the magnetic field.

DC-to-DC converters are being used as ECS of capacitive stationary systems (as described in sections 2.2.2); however, they are not being used in soft robots (as described in sections 2.1) that are typically mobile systems and subject to trade-offs in weight.

We can conclude that a DC-to-DC converter could be used to transfer energy between ICLs for the prolonged power-autonomous operation of ICL robots.

3. Thesis objectives

As we have seen from above, there is a need for implementing proper ECS for ICLs. The current solution is driven such that robot has a single ICL but in case, there would be several, a door to completely new energy management solutions could be opened. Specifically, bidirectional DC-to-DC converters could provide the solution to the energy loss issue: the energy can be transferred from one ICL to another.

Thus, we approached the question about the possibility of increasing energy transfer efficiency between two capacitive robot components. This issue can be circumvented by employing a symmetrical DC-DC converter, which should be designed, taking into account the specific characteristics of our case study – a mobile ICL robot described in Section 2.2.3.

The main requirements of the converter to be developed are as follows:

Low voltage. Relying on the ICL actuator operating voltage, which is about 1V. Commonly, batteries are used as energy sources, but they have very different I-V curves than capacitors, which is our case. Batteries provide a constant voltage, while the voltage of capacitors decreases rapidly during discharge

Multidirectional operation. The proposed converter should be able to transfer energy between multiple ICL capacitors, in all directions (as shown on Figure 2.6)

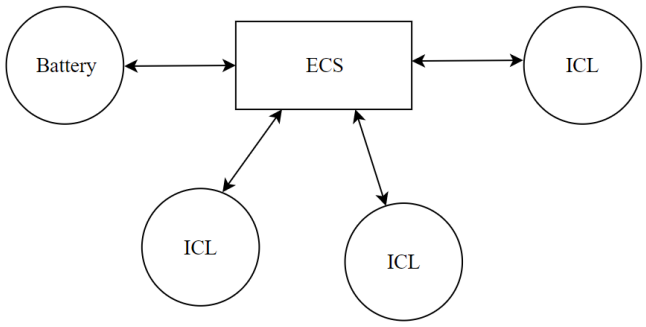

Figure: 2.6 Perspective architecture for energy transfer between ICLs

Bipolar operation. The commercial EDLCs are, as a rule, unipolar devices, so there is no commercial solution optimized for this. The architecture should allow each ICL to be charged in either direction.

3.1. Selected topology

After reviewing the topologies of bidirectional DC-to-DC converters, the buck-boost converter topology was chosen as the optimal configuration due to the following reasons:

1) Functionally, the converter is symmetrical

2) This converter includes only one inductor, which minimizes its size and weight cost.

The main objective of this thesis is to design a symmetrical DC-to-DC converter for capacitive energy swinging. In analogous to a seat often found at playgrounds and other places, the energy swing implies applying an initial impulse to a system that responds by undergoing cyclic motion.

4. Research Methodology

The overall methodology (Chapter 4 and 5) to achieve the proposed solution can be categorized into the following parts:

1. Modeling and optimization of a symmetrical multidirectional buck-boost DC-to-DC converter
2. Converter analysis based on simulations
3. Analysis and Discussion of the designed converter operation (experimental results)

4.1. ICL model

ICL circuit is much more elaborate; but for this work, we use a simplified electrical equivalent circuit described in Section 2.1.2.

First, the working principle of the system (ICL model together with the ECS) is explained followed with the determination of the variables that need to be considered for optimizing the model's efficiency.

4.1.1. Principle of operation

The schematic of the proposed solution is shown in Figure 4.1.

The circuit consists of:

- Two ICLs represented by two capacitors that act as energy source and sink, when the converter operates in a forward direction, and immediately reverse roles when the system operates in the reverse direction.
- Two MOSFETs for switching.
- The inductor as a transmission link between capacitors and acts as an energy storage. This element accumulates energy obtained from source into magnetic field before transferring it to the sink.

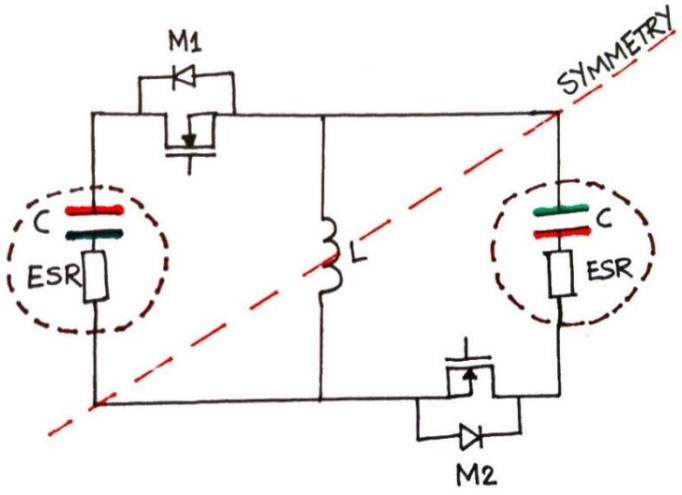

Figure 4.1: Proposed Bidirectional Buck-boost converter

The principle of operation of the proposed system includes the following stages, as shown in figure 4.2, and are explained as follows:

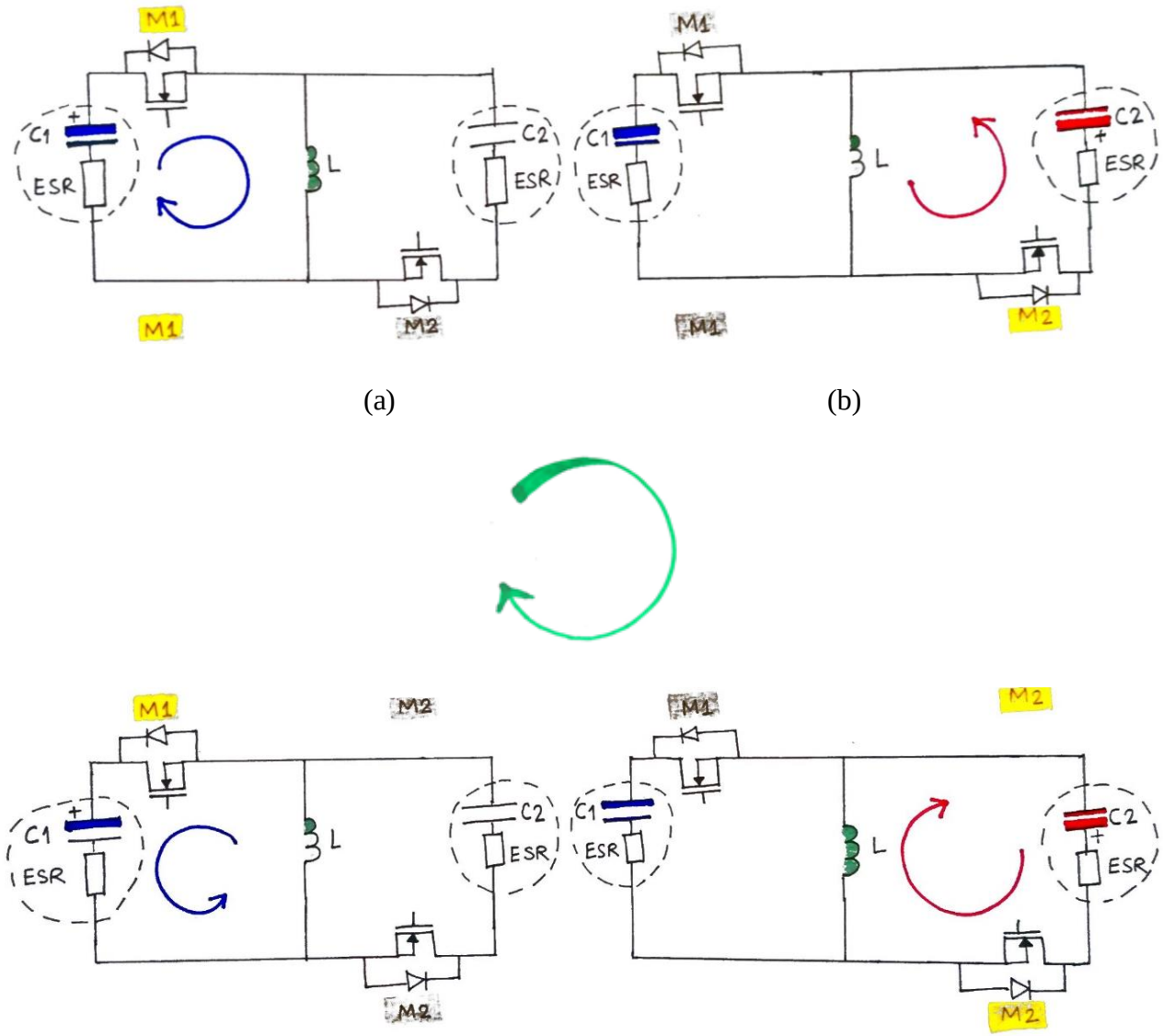

Figure: 4.2 Operation modes of the proposed system.

Blue and Red arrows represent the flow of electrons.

The green arrow represents the sequence of operational steps.

The green color in the inductor shows the amount of accumulated energy.

Forward direction energy transfer.

Stage 1 - Energy accumulation by the inductor.

MOSFET $M_1$is set to "on" condition. During this time, the inductor, receiving current from a capacitor C_1, accumulates energy. At the same time, MOSFET M_2 is in "off" condition and does not pass current (Figure 4.2 (a)).

Stage 2 – Energy transfer to the capacitor C_2.

MOSFET $M_1$is in "off" condition, while the inductor stores energy in the form of magnetic field. The only way for the magnetic energy to be discharged is to transfer it directly to the capacitor C_2 through the MOSFET M_2which is "on", at this time. With no current to sustain the magnetic field, in the inductor, it will collapse and the changing magnetic field will induce a voltage in the opposite direction to the original current. As a result, capacitor C_2 is charged, and has reverse polarity with respect to capacitor C_1 (Figure 4.2 (b)).

Reverse direction energy transfer.

At this step, the energy is transferred in the opposite direction from the capacitor C_2 to capacitor C_1.

Stage 3 - Energy accumulation by the inductor.

First MOSFET M_2 is in the "on" condition, facilitating the transfer of energy from the capacitor $C_2$to the inductor, while MOSFET M_1 is turned "off" (Figure 4.2 (d)).

Stage 4 – Energy transfer to the capacitor C_1.

MOSFET M_1 turns "on" and MOSFET M_2 goes into "off" position, which allows the energy stored in the inductor to be transferred to the capacitor C_1. (Figure 2.2 (c)).

In all stages, the MOSFETs are switched at the moment of reaching a peak energy transfer efficiency.

4.1.2. System modeling and optimization

The input waveforms to DC-to-DC convertor have the following parameters:

- *Switching frequency and inductance*:
  As the switching frequency increases, the minimum size of the inductor to produce continuous current decrease [15]:

$$L_{min} = \frac{(1-D)^2 R}{2f} \tag{4.1}$$

Therefore, high switching frequencies are desirable to reduce the size of both the inductor and the capacitor. The tradeoff for high switching frequencies is increased switching losses. Setting the inductor current variation to 40% of the average inductor current also helps you choose the inductor size, in order to keep the variation small. Typical frequency lies in the range of 20 kHz to overcome audio noise up to 100 kHz to keep switching losses small [15]. We assume an operating frequency of 70 kHz

- *Nonlinear MOSFET capacitances*: - MOSFET has parasitic capacitances: gate-source C_{gs}, gate-drain C_{gd}, drain-source C_{ds} as shown in Figure 4.3.

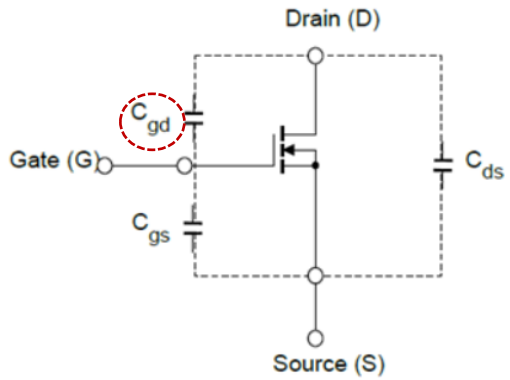

Figure: 4.3 MOSFET capacitances [16].

Usually, it is referring to, as a parasitic capacitance because it limits switching speed [16], but might in our case, it is completely different since voltage-dependent capacitor helping faster energy transfer during the initial phase.

- *Deadtime*: The interval during which both MOSFETs are in the off state is called "Deadtime" [17]. The process of turning on and off the MOSFETs should take place alternatively to prevent latching [18].
- *Duty cycle*: It affects the efficiency of the system.

We will calculate the duty cycle taking into account next assumptions:

- We consider an ideal case, assuming 100% converter efficiency
- The capacitance of both capacitors are equal
- Source capacitor C_1 initially charged and sink capacitor C_2 is uncharged

The energy stored in the capacitor, E_{C1} can be expressed as;

$$E_{c1} = \frac{C_{c1}{U_{c1}}^2}{2} \tag{4.2}$$

Following this, the energy depleted from $E_{C1(depletion)}$,:

$$E_{C1(depletion)} = \frac{E_{C1}}{E_{\max\,(C1)}} * 100\% \tag{4.3}$$

where $E_{\max\,(C1)}$ is the initial energy stored in the capacitor.

Given that efficiency η=100%, we calculate E_{C2} from E_{C1}

$$E_{c2} = E_{\max\,(C1)} - E_{C1} \tag{4.4}$$

And then the voltage in the sink capacitor U_{C2}:

$$U_{C2} = \sqrt{E_{C2} * 2} \tag{4.5}$$

Finally, when we have both U_{C1} and U_{C2}, we can calculate the duty cycle[15]:

$$D = \frac{|U_{C2}|}{(U_{(C1)} + |U_{C2}|)} * 100\% \tag{4.6}$$

Figure 4.4 illustrates the relationship between the duty cycle and voltage at source capacitor C_1.

Figure 4.5 shows the variation of the duty cycle as a function of depletion of energy at C_1.

In our experiments and modeling we made a simplification and operate DC-to-DC converter at a single duty cycle. It has been done for simplicity and a better understanding of the system. Relying on fact, when the voltage level in the capacitor reaches its half of the initial voltage than it already has 75% of energy extracted. So required D lies in the range of values from 0 to 65% (Figure 4.5)

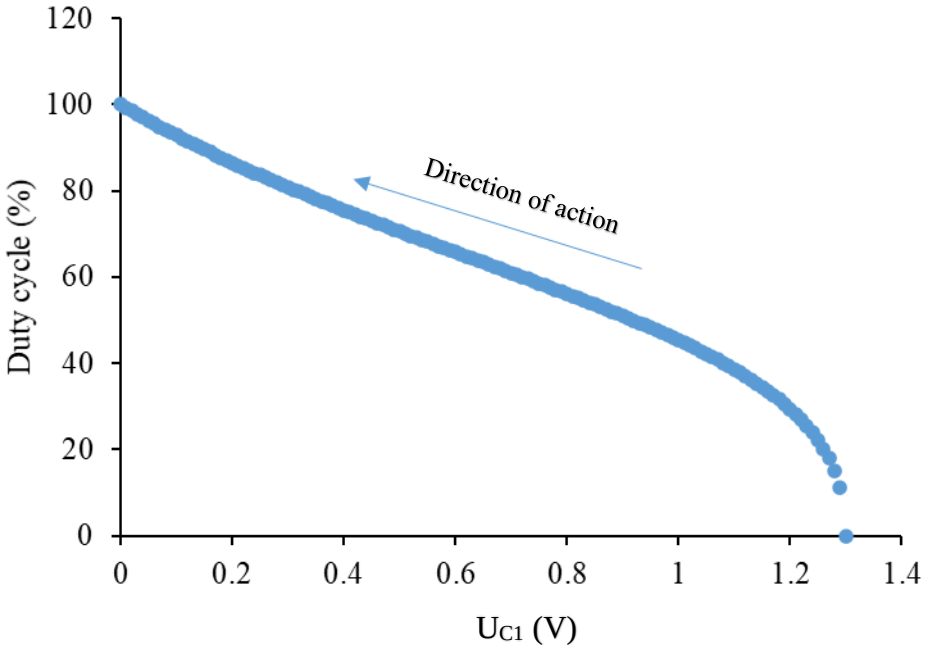

Figure 4.4: Optimal duty cycle versus voltage in C1

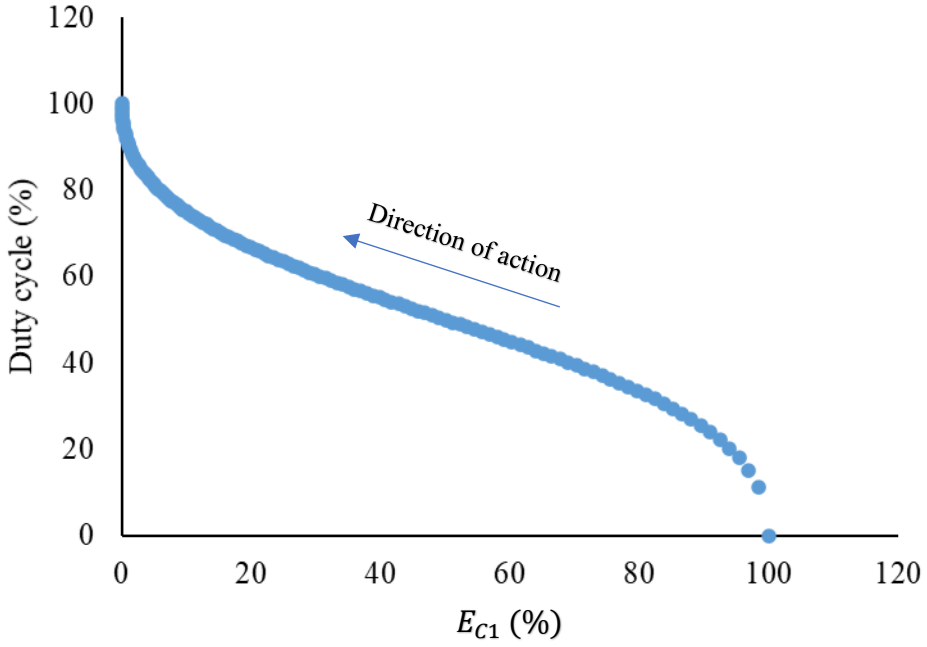

Figure 4.5: Optimal duty cycle versus energy in C1

5. Bidirectional Converter Design

In this chapter, a simplified breadboard is demonstrated along with a discussion and analysis of the obtained results.

5.1. Energy transfer simulation

Based on the optimized parameters considered in Section 4.2 the bidirectional buck-boost convert converter was modeled in the OrCAD and shown in Figure 5.1.

For simplicity and a better understanding of how the converter will behave we start with switch approximation.

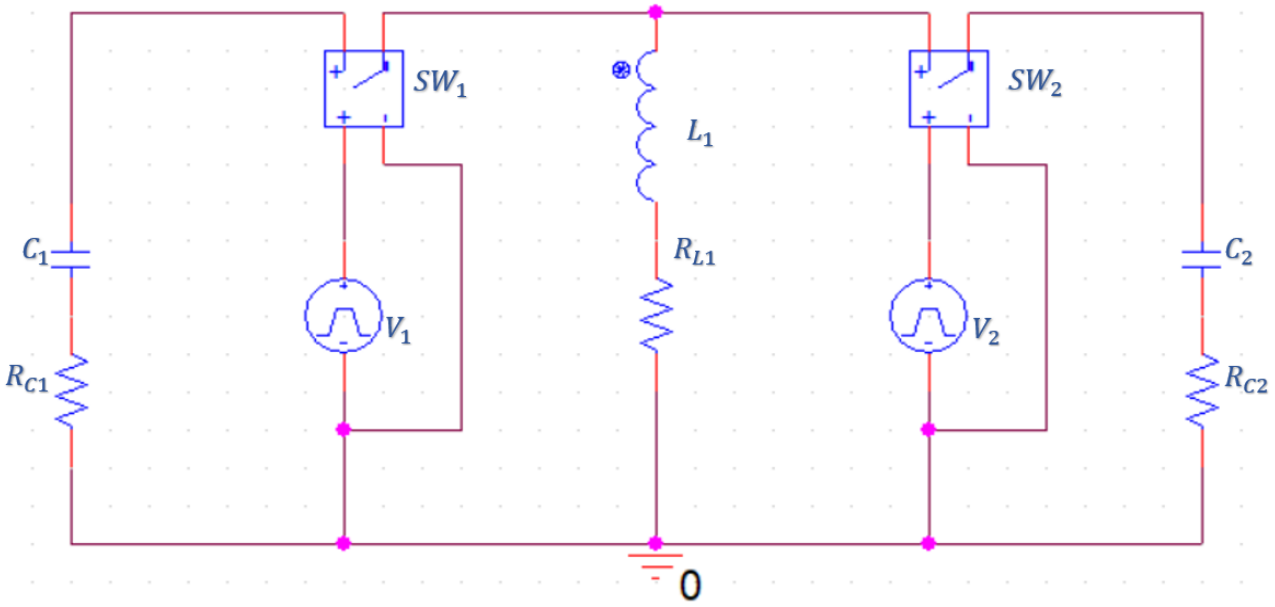

Figure 5.1: Bidirectional Buck-Boost converter topology

The simulation conditions were chosen to simulate the proposed system:

- Two capacitors – (4.7 F with ESR=0.1 Ω) as a model of ICL
- L_1 - inductor 39 μH with low ESR=0.1 Ω, based on the cost of size-weight and calculated minimum inductance (Equation 4.1)
- SW_1, SW_2 - voltage control switch
- V_1, V_2- voltage pulse generator with a rise time t_r and fall time t_f equal to 20 ns

A graph of charge and discharge of the capacitors C_1 and C_2 was simulated for the optimized converter and plotted, as shown in Figure 5.2.

From the graph, we can see the maximum voltage value on C_2 received from C_1, is 0.93 V (which corresponds 71% of the total voltage level in C_1). Moreover, we can observe that the peak value of the transmitted energy is reached after 100 s from the beginning of the simulation.

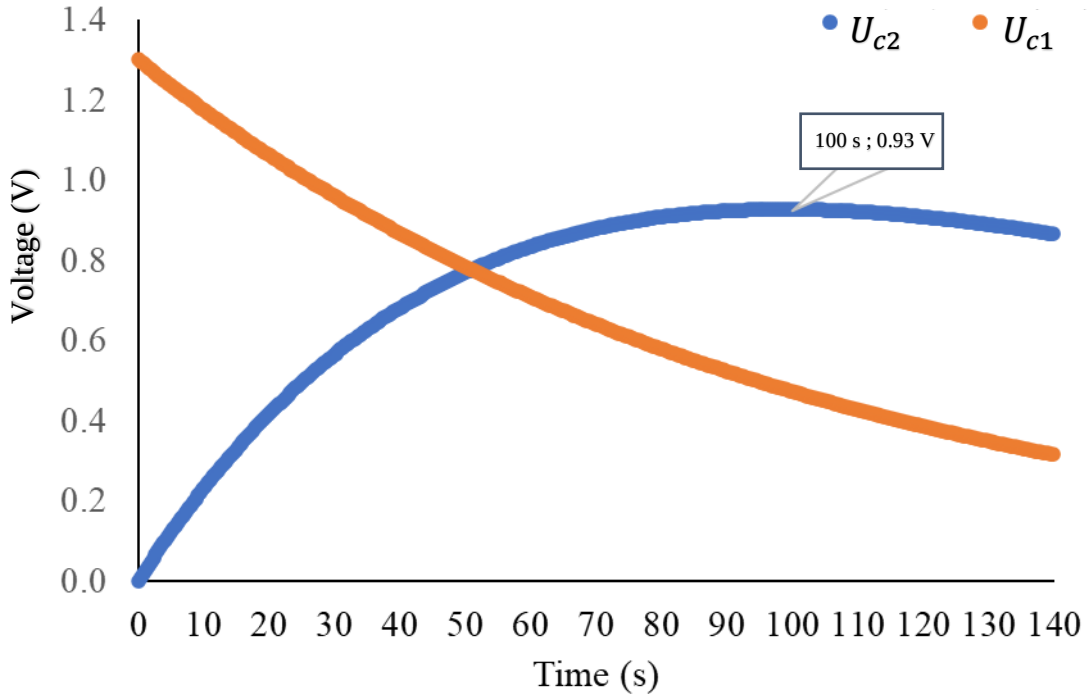

Figure 5.2: Typical capacitor charge-discharge trend

5.2. Breadboard demonstration

Following the analysis of the system in the simulator program, the next step is to set up a breadboard prototype, for evaluating device operability (Figure 5.3.).

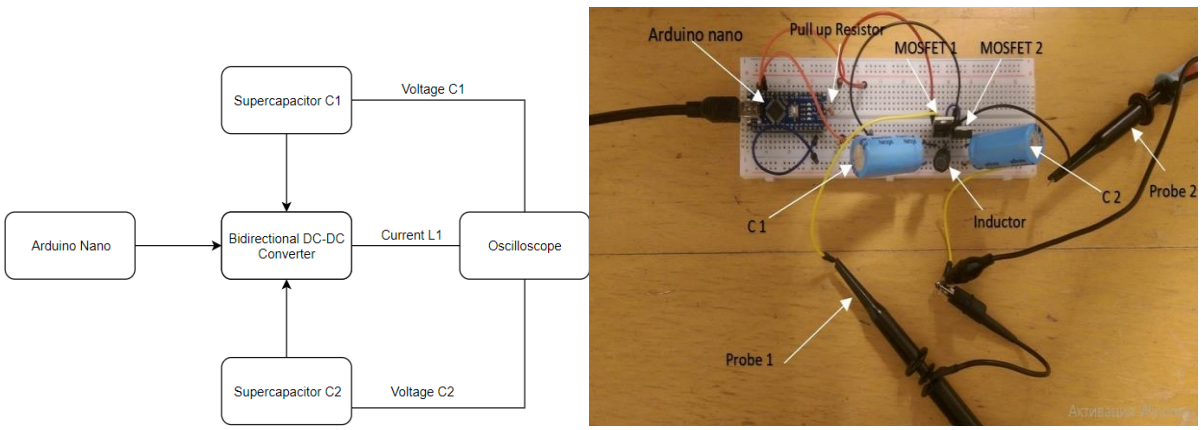

(a) (b)

Figure 5.3 Breadboard evaluation of the Bidirectional DC-to-DC converter. (a) Block diagram; (b) Photo of the set up

The configured system consists of the following components:

- The model of ICL consists of a supercapacitor (4.7 F with ESR=0.1 Ω) in series connection with a resistor (0-4 Ω)
- Inductor 39 μH -nominal value, series RL622 with tolerance 10% [19].
- Arduino Nano - like a pulse width modulation (PWM) generator for MOSFETs control.
- Two MOSFETs IRF3205

The MOSFET was selected as follows:

- The gate-source threshold voltage to open MOSFET should not be higher than 5 V, since this is the maximum amplitude of the signal generated by the Arduino Nano
- On resistance or $R_{DS(on)}$ - should be minimal, since it will provide switching energy loss

5.3. Designed converter operation analysis

5.3.1. Forward directional operation

First, an experiment was conducted on the operation of the system in the forward transfer operation. From the obtained results (Figure 5.4) we see that the maximum voltage on the capacitor C_2 equal to 0.92 V (which corresponds 70.8% from the total voltage level in C_1) and achieved after 100 s from the moment the experiment begins.

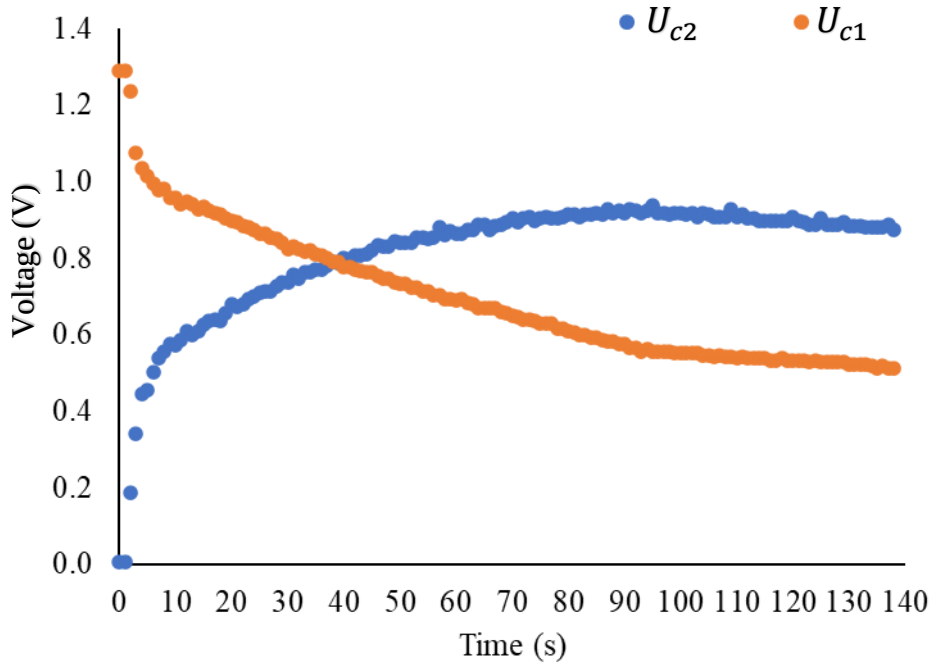

Figure 5.4: Voltage transfer between capacitors

The process of discharging the C_1, and C_2, (Eq.4.2) is used to determine the amount of transferred energy. The corresponding graph is also shown (Figure 5.5). We can see that when 100s is reached from the beginning of the experiment, the peak of transferred energy occurs, and it is equal to 1.9 J

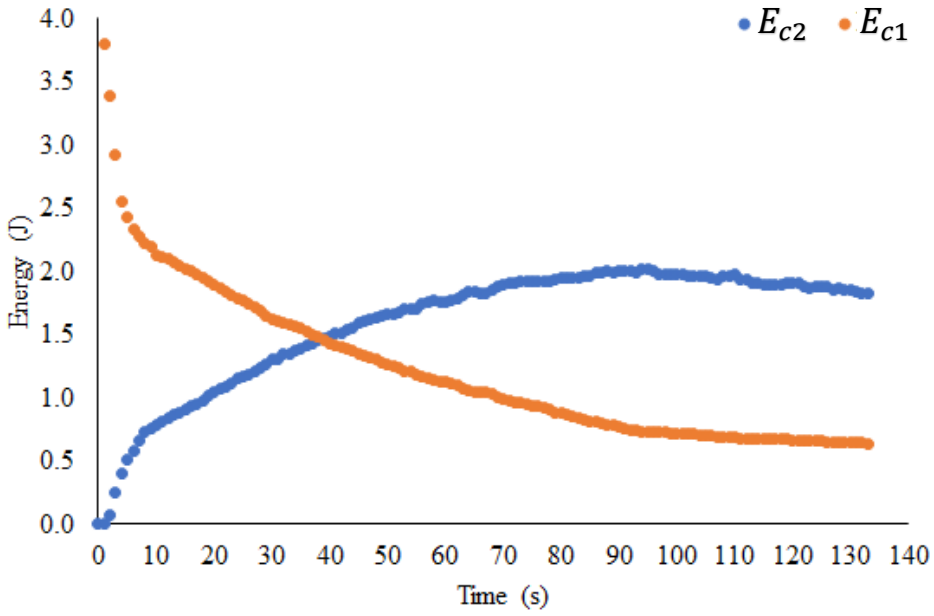

Figure 5.5: Energy transfer between capacitors

For determining the energy conduction mode at which our experimental set up operates. We measured current on the inductor and voltage across both capacitors at different time steps (Figure 5.6)

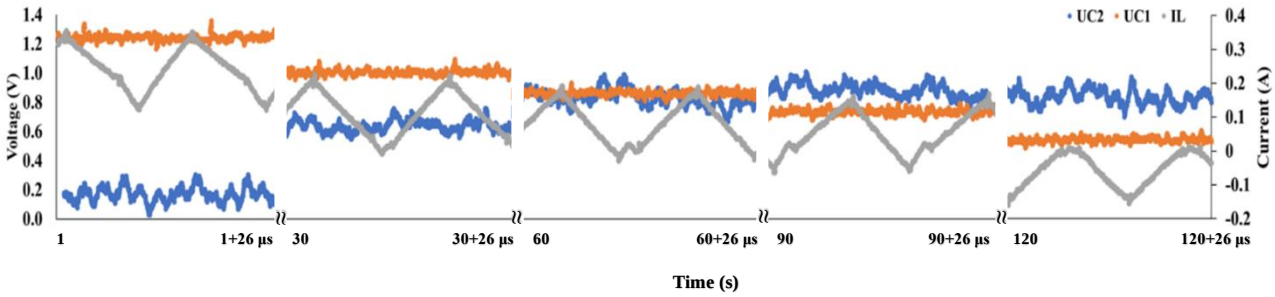

Figure 5.6: Current at different time steps: Experiment

Initially (around 1 s), the energy transfer process takes place in Continuous Conduction Mode (CCM) which happens when the inductor's current does not reach zero. This occurs since capacitor C2 is completely discharged. With an increase in voltage across C2 and respectively decreasing in C1, the trough of the ripple current touched zero and the energy transfer process goes to Discontinuous Condition Mode (DCM) (around 30 s). However, when the converter has two MOSFETs, like in our case, it is operating under light conditions and the current goes negative (around 90 s) [20].

5.3.2. Converter efficiency concept and analysis

With obtained data about energy transfer, the next step was the calculation of converter efficiency. In case when the final energy of source is neglected, we consider the energy of the sink capacitor at every instant divided by the source capacitor at an initial instant:

$$(\eta_{cumul})_{t=i..n} = \frac{(Energy\ sink)_{(t_{i..n})}}{(Energy\ Source)_{t_i}} * 100\% \tag{5.1}$$

i- is the first instant and n- is every instant

However, in the case of bidirectional energy transfer, we do not have to neglect the final energy of the source capacitor. Since we can push and pull the charge between two capacitors for a large number of times and this suggests that not worth to completely discharge our source capacitor. Nevertheless, one reason we are interested in discharging the capacitor as completely as possible, based on the charge-energy relation. When the charge in the capacitor reaches half of its initial charge, we will actuate 50% of charge, but already spent 75% of energy. Consequently, we have a trade-off between the left 50% of actuation and 25% of energy.

When the final energy of source is not neglected, we take the energy of the sink capacitor at a previous instant and divide it by the energy of the source capacitor at that instant:

$$(\eta_{diff})_{t=i..n} = \frac{(Energy\ accumulated)_{(t=i..n)}}{(Energy\ depleted)_{(t=i..n)}} * 100\%$$

$$\Rightarrow (\eta_{diff})_{t=i..n} = \frac{(Energy\ sink)_{[(t_i-(t_i-1))..(t_n-(t_n-1))]}}{(Energy\ Source)_{[(t_i-(t_i-1))..(t_n-(t_n-1))]}} * 100\% \tag{5.2}$$

Based on (Eq.5.1), efficiency was calculated after conducting a series of experiments with different frequencies 67 kHz, 77 kHz, 90 kHz to analyze the effect of frequency on system performance. We can see higher efficiency with a frequency of 77 kHz. The maximum peak efficiency of the system reached is 50% (Figure 5.7).

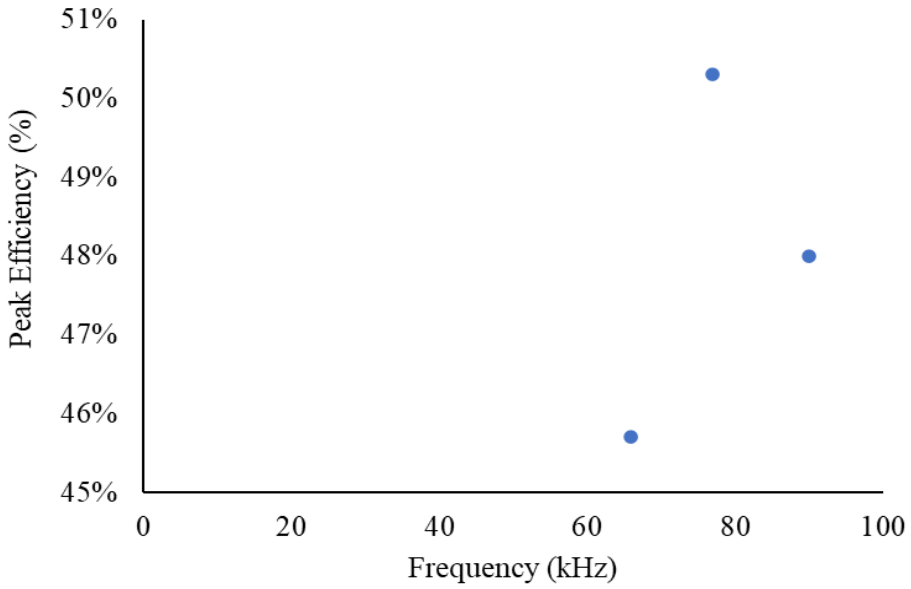

Figure 5.7: Efficiency vs frequency.

The next step was a comparison of the energy transfer efficiency in the case of the experiment and simulation with switch approximation (Figure 5.8).

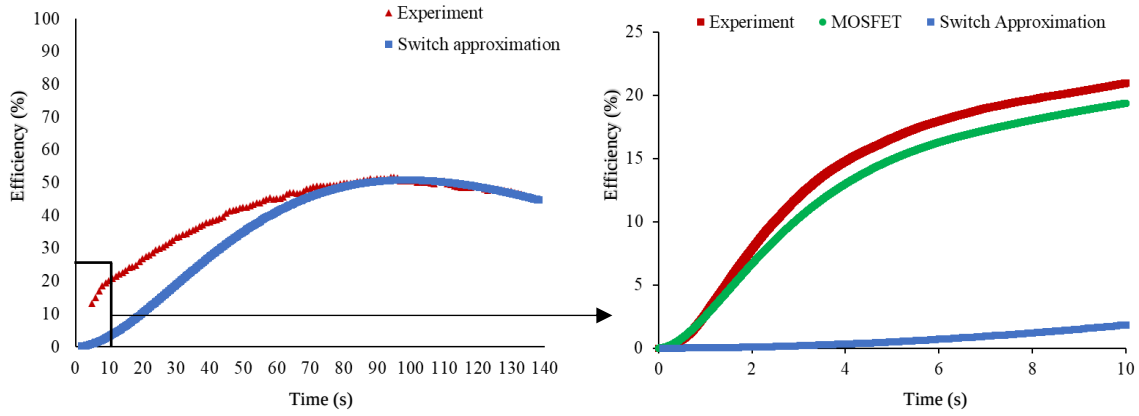

Figure 5.8: Efficiency Comparison: Switch approximation and Experiment

The maximum efficiency in the case of the experimental part is 50.3%, while the simulation with switch approximation reaches a value of 50.8%. From the simulation we see convergence closer to reaching peak efficiency. However, we also have a discrepancy in the initial phase.

To explain this difference, another simulation was conducted in Pspice taking into account the MOSFET IRF3205 used in our experiment. As a result, we see convergence in the initial phase between the experiment and the simulation with the MOSFET (Figure 5.8).

A comparison was also made between simulation with switch approximation and experiment regarding energy depletion and accumulation between capacitors. Initially C_1, had 3.9 J as can be

seen from Figure 5.9. Amount of accumulated energy in C_2, in case of simulation and experiment is almost the same (close to 2 J).

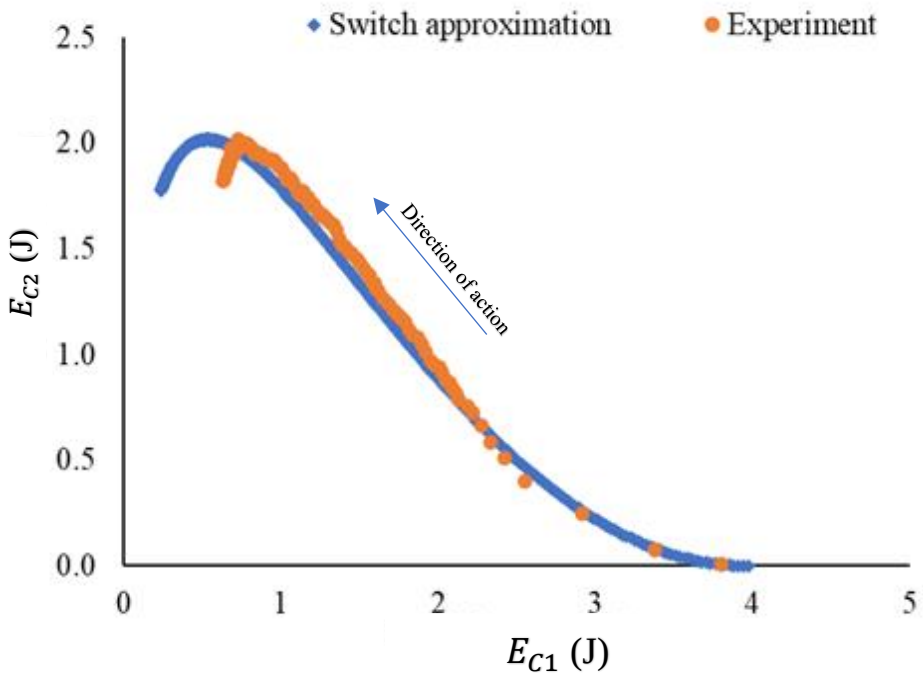

Figure 5.9: Correlation of energy accumulation and depletion: Experiment and Switch approximation

As a next step, efficiency was calculated based on (Eq.5.2), and convergence comparison was made

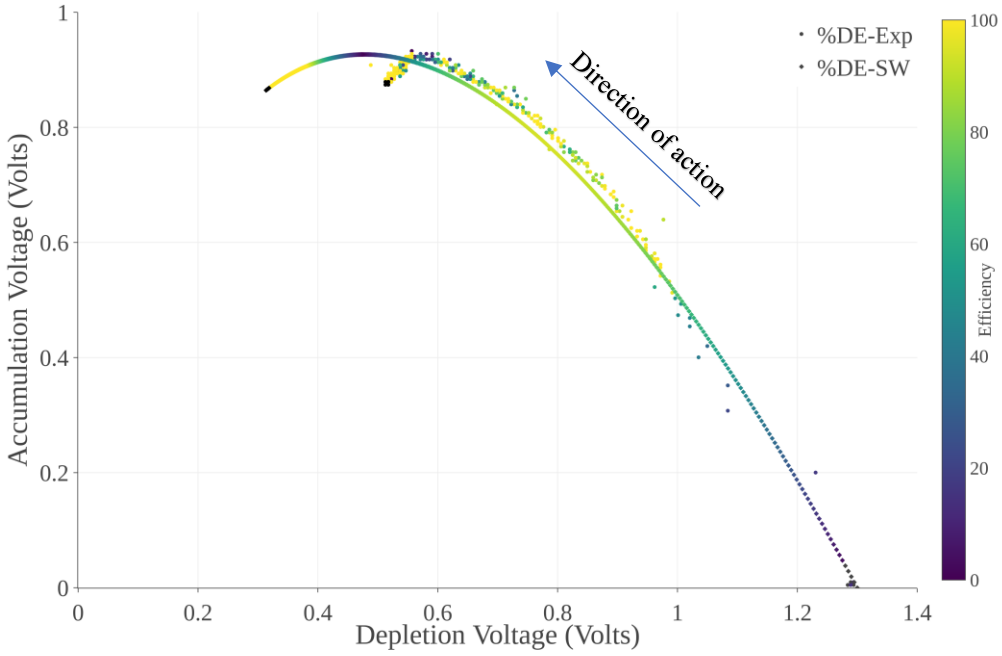

Figure 5.10: Efficiency Convergence: Experiment and Simulation

From the graph we can see high convergence after 0.8 V from the beginning of transfer operation. The efficiency at the same range, represented by the color bar, reaches approximately 99%.

However, it does not converge well in the initial phase, because the switch does not have a real representation of the MOSFET. It does not have a junction capacitance, as a MOSFET does.

5.3.3. Bidirectional operation

Graphs (5.11-5.13) represent forward and reverse energy transfer operation as one single mode.

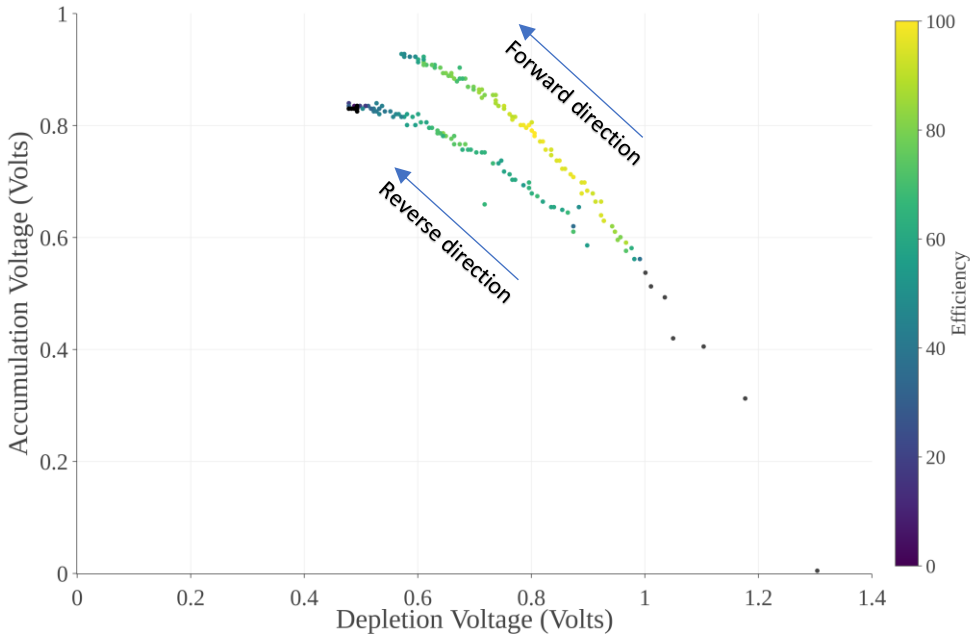

Figure 5.11: Efficiency variation in Bidirectional mode (R=0 Ω).

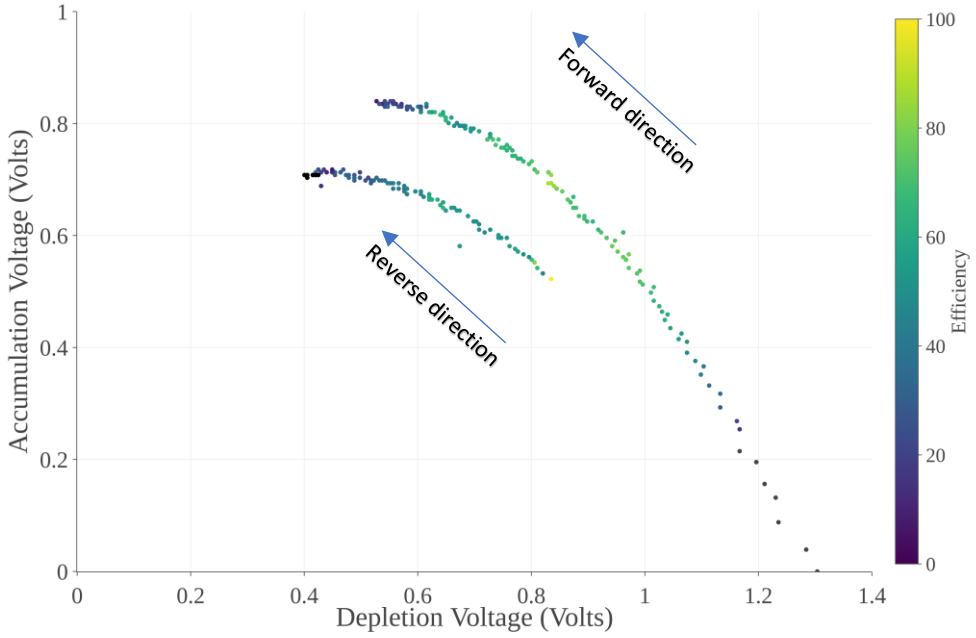

Figure 5.12: Efficiency variation in Bidirectional mode (R=2 Ω).

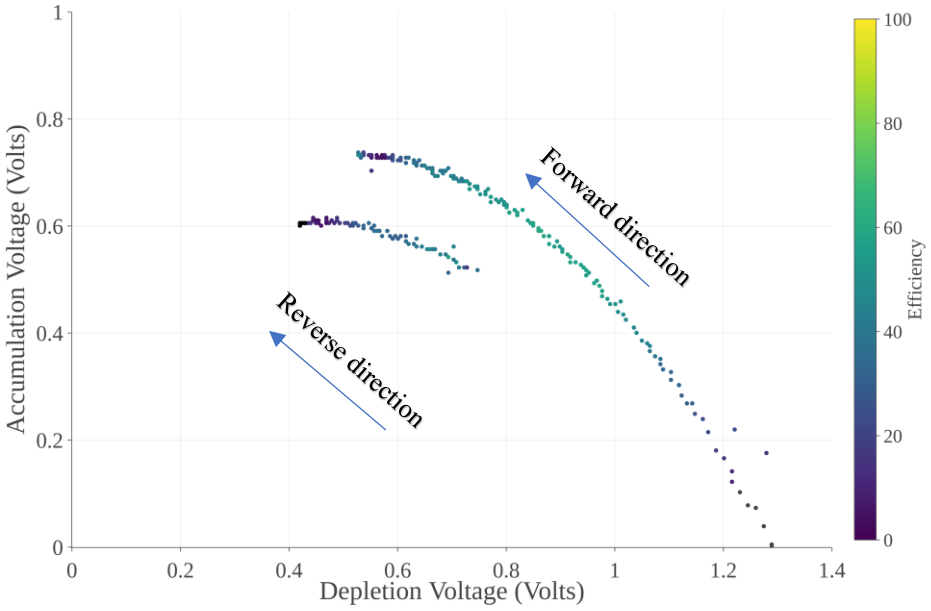

Figure 5.13: Efficiency variation in Bidirectional mode (R=4 Ω).

First, we start the extraction of energy from the capacitor $C_1$to capacitor C_2 in the forward direction. At some point when it reaches maximum efficiency, it settled a bit, and then starts reverse energy transfer operation, between C_2 and C_1. From that moment capacitor C_2 gives energy to C_1. Efficiency at the end for the forward and beginning of the reverse direction transfer almost at the same range. Also, from the graph we can conclude that the most efficient energy transfer region, represented by a color bar, lies in the range from 1 V to 0.7 V after the beginning of the transition in a forward direction and reaches approximately 99%. However, with increasing resistance in the system with the step of 2 Ω, the range with the highest efficiency remains the same, but overall the efficiency decreases by about 20%.

6. Conclusion and Future perspectives

The results obtained by the study support the proposed solution and confirm the possibility of increasing energy transfer efficiency between two identical capacitors, by implementing the designed symmetrical DC-to-DC buck-boost converter.

The proposed solution has been developed considering the specific characteristics of the application case scenario, ICL robot, and can provide energy transfer operation in both directions between capacitors, with voltage level about 1 V.

Modeling and simulation of the proposed solution were done in the OrCAD Pspice program. Following this, an energy transfer efficiency equal to 50.3% was demonstrated with the help of a breadboard set-up.

A high convergence between the experimental and simulation efficiency results was observed, with the separation during the initial phase of the energy transfer process. Such a deviation was present due to the use of switch approximation. As a result, MOSFET modeling was tuned to minimize the preexisting difference and to improve convergence at the initial stage of charging.

By calculating the efficiency of the system, taking into account the final energy of the source capacitor, the optimal operating range for energy transfer was determined, which lies in the range of 1 V to 0.7 V.

The proposed solution proved its 50.3% efficiency. In the future, the system will be improved in the following aspects:

- Implement an improved MOSFET model.
- Implement a Maximum Power Point Tracking (MPPT) control, which should help to increase the efficiency of energy transfer.
- Extension of the system architecture for connecting an arbitrary number of supercapacitors.

References

[1] C. Laschi and M. Cianchetti, “Soft Robotics : New Perspectives for Robot Bodyware and Control Soft robotics : new perspectives for robot bodyware and control,” vol. 2, no. August, pp. 1–5, 2014, doi: 10.3389/fbioe.2014.00003.

[2] F. Iida and C. Laschi, “Soft Robotics : Challenges and Perspectives,” vol. 7, pp. 99–102, 2011, doi: 10.1016/j.procs.2011.12.030.

[3] “Why Do We Need Soft Robotics? | RobotShop Community.” Accesssed on: May 18, 2020.[Online].Avaliable: https://www.robotshop.com/community/blog/show/why-do-we-need-soft-robotics

[4] F. Schmitt, O. Piccin, L. Barbé, and B. Bayle, “Soft robots manufacturing: A review,” *Front. Robot. AI*, vol. 5, pp. 1–17, 2018, doi: 10.3389/frobt.2018.00084.

[5] F. Kaasik *et al.*, “Scalable fabrication of ionic and capacitive laminate actuators for soft robotics,” *Sensors Actuators, B Chem.*, vol. 246, pp. 154–163, 2017, doi: 10.1016/j.snb.2017.02.065.

[6] I.Must, Ionic and capacitive electroactive laminates with carbonaceous electrodes as sensors and energy harvesters. Ph.D. dissertation, Institute of Technology, University of Tartu, Estonia, 2014.

[7] I. Must *et al.*, “Ionic and capacitive artificial muscle for biomimetic soft robotics,” *Adv. Eng. Mater.*, vol. 17, no. 1, pp. 84–94, 2015, doi: 10.1002/adem.201400246.

[8] S. A. Gorji, H. G. Sahebi, M. Ektesabi, and A. B. Rad, “Topologies and control schemes of bidirectional DC–DC power converters: An overview,” *IEEE Access*, vol. 7, pp. 117997–118019, 2019, doi: 10.1109/ACCESS.2019.2937239.

[9] F. Caricchi, F. Crescimbini, G. Noia, and D. Pirolo, “Experimental study of a bidirectional dc-dc converter for the dc link voltage control and the regenerative braking in pm motor drives devoted to electrical vehicles,” vol 1, pp. 381–386, 1994.

[10] H. Matsuo and F. Kurokawa, "New Solar Cell Power Supply System Using a Boost Type Bidirectinal DC-DC Converter," in IEEE Transactions on Industrial Electronics, vol. IE-31, no. 1, pp. 51-55, Feb. 1984, doi: 10.1109/TIE.1984.350020.

[11] [10]K. Tytelmaier, O. Husev, O. Veligorskyi and R. Yershov, "A review of non-isolated bidirectional dc-dc converters for energy storage systems," 2016 II International Young Scientists Forum on Applied Physics and Engineering (YSF), Kharkiv, 2016, pp. 22-28, doi: 10.1109/YSF.2016.7753752.

[12] “Different Types of DC-DC Converters and Its Advantages.” Accessed on May 20, 2020.[Online].Avaliable: https://www.elprocus.com/different-types-dc-to-dc-converters/

[13] “Introduction to DC-DC Converters.” Accesssed on: May 20, 2020.[Online].Avaliable: https://www.digikey.com/en/maker/blogs/introduction-to-dc-dc-converters

[14] A. K. Singal, "The paradox of two charged capacitors - a new perspective", Physics Education, vol. 31, no. 4, pp. 1-13, 2015.

[15] W. Hart Danial, *Power Electronics*. McGraw-Hill, 2010.

[16] N. Caka, M. Zabeli, M. Limani, and Q. Kabashi, “Influence of MOFSET parameters in its parasitic capacitances and their impact in digital circuits,” *WSEAS Trans. Circuits Syst.*, vol. 6, no. 3, pp. 281–287, 2007.

[17] “Dead Time Losses in Synchronous Rectifying Step-Down Converters | Basic Knowledge |

ROHM TECH WEB: Technical Information Site of Power Supply Design.” Accesssed on: May 1, 2020.[Online].Avaliable: https://techweb.rohm.com/knowledge/dcdc/dcdc_sr/dcdc_sr02/6997

[18] Y. Zhang and J. Wang, “Understanding Dead-time Based On TPS51225/275/285 Application Report Understanding Dead-time Based On TPS51225/275/285,” 2018. Accessed: Apr. 30, 2020. [Online]. Available: www.ti.com.

[19] Bourns, “RL622 Series - Radial Lead RF Choke,” 2011.[Online]. Avaliable: https://www.bourns.com/docs/Product-Datasheets/rl622_series.pdf Accessed: 2020-05-19

[20] Paul M. Muchinsky, *Power Supplies Explained*. Radio Society of Great Britain, 2018.

Non-exclusive licence to reproduce thesis and make thesis public

I, Oleksandr Syzoniuk

1. herewith grant the University of Tartu a free permit (non-exclusive licence) to:

1.1. reproduce, for the purpose of preservation, including for adding to the DSpace digital archives until the expiry of the term of copyright, and

1.2. make available to the public via the web environment of the University of Tartu, including via the DSpace digital archives, under the Creative Commons licence CC BY NC ND 3.0, which allows, by giving appropriate credit to the author, to reproduce, distribute the work and communicate it to the public, and prohibits the creation of derivative works and any commercial use of the work from ***20/05/2023*** until the expiry of the term of copyright,

"**A symmetrical dc-to-dc converter for capacitive energy swinging**"

supervised by **Indrek Must** and **Saoni Banerji**

2. I am aware of the fact that the author retains the rights specified in p. 1.

3. I certify that granting the non-exclusive licence does not infringe other persons' intellectual property rights or rights arising from the personal data protection legislation.

Oleksandr Syzoniuk
20/05/2020